NUMERICAL SIMULATION OF FREE CONVECTION IN A 3D ENCLOSURE FILLED WITH HYBRID-NANOFLUID AND SATURATED PARTIALLY WITH POROUS MEDIUM, UNDER MAGNETIC FIELD INFLUENCE

Younus JANABI[1*], Tudor PRISECARU[2], Valentin APOSTOL[3]

A numerical simulation of natural convection inside a cubical enclosure filled with hybrid nanofluid (Al_2O_3-Cu/water) and partially saturated with porous medium has been investigated. Navier-Stoke equations are used to simulate the convection heat transfer for the hybrid-nanofluid layer, while the governing equation in porous media is solved by using the Darcy-Brinkmann model. Numerical solutions are obtained employing FEM. Key parameters are studied under different ranges, such as the Rayleigh number, Hartmann number, Darcy number, solid volume fraction of nanoparticles, and porosity of the porous layer. Results showed that as the magnetic field increases from Hartmann number (Ha = 40 to 60), the solid volume percentage of the nanoparticles slightly affects the temperature. Moreover, the Nusselt number is inversely proportional to the Hartmann number and directly proportional to the solid volume fraction, nanoparticle concentration, and the Rayleigh number.

Keywords: Free convection, cubical enclosure porous medium, hybrid nanofluid, magnetic field effect

1. Introduction

In the past few years, authors have concentrated on improving heat transfer in industrial applications. Most of the applications use pure fluids, like oil, ethylene glycol, and water, as liquid cooling, which do not have high heat conductivity, which restricts the improvement in the rate of thermal transfer [1]**.** Using novel methods, such as hybrid nanofluids with porous mediums, improves thermal efficiency. Nano-fluid is defined as a mixture of based fluid and dispersed nanometers, which was presented for the first time by Choi [2]. The purpose of this mixing is to develop thermal transport fluids with significant conductivities. The investigation of convection heat transfer inside an enclosure employing porous media is a crucial problem in numerous industrial engineering applications, like cooling computer systems, ground-coupled heat pumps, heat exchangers, electronic equipment, and solar collectors. M. Hemmat Esfe et al. [3] implemented numerical simulations to study 3D free convection flow inside a

[1] PhD Student, University POLITEHNICA Bucharest, Department of Thermotechnics, Thermal Machines and Refrigeration Systems, e-mail: janabi90@gmail.com (corresponding authors)
[2] Prof., University POLITEHNICA Bucharest, Department of Thermotechnics, Thermal Machines and Refrigeration Systems, e-mail: tudor.prisecaru@upb.ro
[3] Prof., University POLITEHNICA Bucharest, Department of Thermotechnics, Thermal Machines and Refrigeration Systems, e-mail: valentin.apostol@upb.ro

cubical enclosure saturated with nanofluid (CuO-water and equipped with a porous fin. They found that the Nusselt number and heat transfer improved by increasing the volume concentration of nanoparticles**.** Venkatadri et al. [4] provided a deep examination of the natural convection of nanofluid flow inside a trapezoidal enclosure that is filled with a porous. They observed that as the Rayleigh number and volume fraction increase, it leads to an increase in the Nusselt number.

Abderrahmane et al. [5] carried out 3D free convection of Darcy porous rectangular wavy enclosure encompassing nanofluid (Fe_3O_4-water) in the presence of magnetic field. The outcomes revealed that utilizing a MF in the enclosure reduces the Nusselt number. Hartmann numbers have a negative impact on the rate of thermal transfer of around 15%. It was observed that rising the Darcy number and Rayleigh number leads to an elevation in the Nusselt number Muhammad and Naveed [6] proved an analytical study of the magnetohydrodynamic flow of Al_2O_3-ethylene glycol nanofluid in a rectangular enclosure with expanding porous walls. It was noticed that the aggregation of Al_2O_3 nanoparticles impacts and sometimes inhibits the fluctuations brought on by other variables. Abdelraheem M. Aly [7], simulated free convection within a circular enclosure filled with nanofluid porous media. As the porous layer radius, inner square length, and volume fraction increase, the Nusselt number reduces**.** Al-Amir et al. [8] studied natural HT and entropy generation in a corrugated Z-shape enclosure saturated with TiO_2-water nanofluid and porous medium. They observed that the Nusselt number reduces to 30% with rising heat generation. The heat transfer increased to 80% with increasing Ra (10^5 to 10^6). Reddy et al. [9] examined MHD convection heat transfer in a tilt annulus saturated with hybrid nonliquid and porous mediums. It has been observed that raising the Darcy number drives an improvement in the average Nusselt number.

To the best of our knowledge, no literature has been reported on the effect of the four-heating block on laminar free convection inside the cubical enclosure filled with hybrid nanofluid and partially saturated with porous medium. Investigations are performed for various values of the parameters, including porosity, solid volume percentage, nanoparticle concentration, Rayleigh number, and Hartmann number. Furthermore, an analysis is conducted between three different thicknesses of porous layers to study the effects on flow and heat transfer inside the enclosure.

2. Physical problem model

The configuration considered for this study is depicted in Fig.1. The investigation involves a study of laminar natural convection heat transfer flow within a 3-dimensional cubical enclosure filled with a hybrid nanofluid (Al_2O_3-Cu/Water), partially saturated with porous medium, and heated by four heating

blocks. Based on the following presumptions, the governing system is developed. The four sources are integrated on the right upper and lower vertical walls, as well as on the upper and lower left vertical walls of the enclosure and kept at a high temperature. The front and back walls are at a low temperature, while the other walls are adiabatic. The L, W, and H dimensions of the enclosure and heating sources are indicated, respectively. The hybrid layer is on the left, while the porous layer is on the right. The fluid in the enclosure consists of two layers: the first right layer is porous medium, while the second left layer is hybrid nanofluid. In this model, three different thicknesses are examined for porous medium. The interface between the hybrid nanofluid and porous medium is permeable. The layers of porous medium are saturated with the same hybrid nanofluid. The magnetic field is supplied horizontally without an inclination angle along the x-axis. The parameters used for studying in current model are Rayleigh number $10^3 \leq$ Ra $\leq, 10^6$, Prandtl number 6.2, permeability 0.4, Darcy number $10^{-5} \leq$ Da $\leq 10^{-1}$, volume fraction of concentration nanoparticles $0 \leq \emptyset \leq 0.1$, and Hartmann number $0 \leq$ Ha ≤ 60. The finite element is utilized to discretize the governing equations. The flow is considered steady, three- dimensional, incompressible, and laminar. Radiation effects on heat transfer are considered negligible. At the walls, non-slip conditions have been implemented. The base fluid and nanoparticles are mixed to form a homogeneous mixture in the local thermal equilibrium. The thermophysical properties of pure water and nanoparticles are shown in the (Table 1), except for density, which is determined based on the Boussinesq approximation. Furthermore, the interface between the nanofluid and porous medium layers is assumed to be permeable. In this study, classical Darcy's law may not provide a comprehensive understanding of the behavior of fluid flow in the porous layer. Therefore, the Brinkman-extended non-Darcy model is utilized to model the porous layer.

Table 1

Thermophysical properties of pure water and nanoparticles [10]

Properties	Water	Copper (Al_2O_3)	Alumina (Cu)
ρ [kg/m^3]	998.2	3970	8933
k [W/(m.K)]	0.613	40	400
cp [J/(kg.K)]	4182	765	385
β [1/K]	21×10^{-5}	2.55×10^{-5}	5×10^{-5}

The governing equations of the fluid flow and heat transfer problems are indeed based upon the three fundamental laws of physics: the continuity equation, the momentum equation, and the energy equation. Navier-Stoke equations were used to simulate the convection heat transfer for the nanofluid layer, while the governing equation in the porous slab was solved using the Darcy-Brinkmann

model. In the present application, the models for fluid flow and heat transfer are solved numerically using the finite element method.

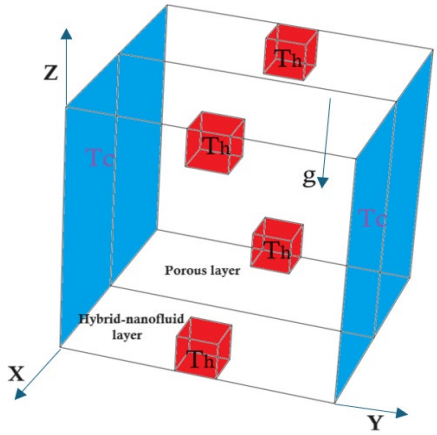

Fig.1: Schematic diagram of the current study

3. Governing equations

Under these assumptions the governing equation can be written as follows: **Thirupati et al. [11].**

Continuity equation

$$\frac{\partial u}{\partial x}+\frac{\partial v}{\partial y}+\frac{\partial w}{\partial z}=0 \tag{1}$$

Momentum-X

$$u\frac{\partial u}{\partial x}+v\frac{\partial u}{\partial y}+w\frac{\partial u}{\partial z}=-\frac{1}{\rho_{hnf}}\frac{\partial p}{\partial x}+\mu_{hnf}\left(\frac{\partial^2 u}{\partial x^2}+\frac{\partial^2 u}{\partial y^2}+\frac{\partial^2 u}{\partial z^2}\right)-(C_2\mu_{hnf}\frac{u}{k}) \tag{2}$$

Momentum-Y

$$\text{Y}\quad u\frac{\partial v}{\partial x}+v\frac{\partial v}{\partial y}+w\frac{\partial v}{\partial z}=-\frac{1}{\rho_{hnf}}\frac{\partial p}{\partial y}+\mu_{hnf}\left(\frac{\partial^2 v}{\partial x^2}+\frac{\partial^2 v}{\partial y^2}+\frac{\partial^2 v}{\partial z^2}\right)-\ (C_2\mu_{hnf}\frac{v}{k}) \tag{3}$$

Momentum -Z

$$u\frac{\partial w}{\partial x}+v\frac{\partial w}{\partial y}+w\frac{\partial w}{\partial z}=-\frac{1}{\rho_{hnf}}\frac{\partial p}{\partial z}+\mu_{hnf}\left(\frac{\partial^2 w}{\partial x^2}+\frac{\partial^2 w}{\partial y^2}+\frac{\partial^2 w}{\partial z^2}\right)+\frac{(\rho*\beta)_{hnf}}{\rho_{hnf}}*g*(T-T_c)+\frac{B_o^2\ \sigma_{hnf}}{\rho_{hnf}}-C_2\mu_{hnf}\frac{w}{k} \tag{4}$$

Energy equation

$$(\rho c_p)_f\frac{\partial T}{\partial t}+(\rho c_p)_{hnf}\ (u\frac{\partial T}{\partial x}+v\frac{\partial T}{\partial y}+w\frac{\partial T}{\partial z}=\alpha^*\left(\frac{\partial^2 T}{\partial x^2}+\frac{\partial^2 T}{\partial y^2}+\frac{\partial^2 T}{\partial z^2}\right) \tag{5}$$

$$C2=\begin{cases}0, & only\ hybrid-nanofluid\\ 1, & hybrid\ nanofluid\ with\ porous\end{cases}$$

$$\alpha^*=\begin{cases}\alpha_{hnf}, & only\ hybrid-nanofluid\\ \alpha_{eff}, & hybrid\ nanofluid\ with\ porous\end{cases}$$

The dimensionless form of the governing equations can be formulated as follows by using the dimensionless parameters.

$$X=\frac{x}{H},Y=\frac{y}{H},Z,=\frac{z}{Y},U=\frac{uH}{\alpha_f},V=\frac{vH}{\alpha_f},W=\frac{wH}{\alpha_f},Pr=\frac{v_f}{\alpha_f},P=\frac{pH^2}{\rho_{hnf}\alpha_f^2},\theta=\frac{T-T_c}{T_h-T_c},Ra=$$
$$g\beta_f(T_h-T_c)/(v_f*\alpha_f),Ha=HB_o\sqrt{(\frac{\sigma_{hnf)}}{\rho_{hnf}v_{hnf}}},Da=\frac{k}{H^2},$$

(6)

$$\frac{\partial u}{\partial x}+\frac{\partial v}{\partial y}+\frac{\partial w}{\partial z}=0 \quad (7)$$

$$U\frac{\partial U}{\partial X}+V\frac{\partial U}{\partial Y}+W\frac{\partial U}{\partial Z}=-\frac{\rho_f}{\rho_{hnf}}\frac{\partial P}{\partial X}+\frac{\mu_{hnf}}{\rho_{hnf}\alpha_f}\left(\frac{\partial^2 U}{\partial X^2}+\frac{\partial^2 U}{\partial Y^2}+\frac{\partial^2 U}{\partial Z^2}\right)-C_2(\frac{\mu_{hnf}}{\rho_{hnf}\alpha_f}\frac{U}{Da}) \quad (8)$$

$$U\frac{\partial V}{\partial x}+V\frac{\partial V}{\partial y}+W\frac{\partial V}{\partial z}=-\frac{\rho_f}{\rho_{hnf}}\frac{\partial P}{\partial Y}+\frac{\mu_{hnf}}{\rho_{hnf}\alpha_f}\left(\frac{\partial^2 V}{\partial X^2}+\frac{\partial^2 V}{\partial Y^2}+\frac{\partial^2 V}{\partial Z^2}\right)-C_2(\frac{\mu_{hnf}}{\rho_{hnf}\alpha_f}\frac{V}{Da}) \quad (9)$$

$$u\frac{\partial W}{\partial x}+v\frac{\partial W}{\partial y}+W\frac{\partial W}{\partial z}=-\frac{\rho_f}{\rho_{hnf}}\frac{\partial P}{\partial Z}+\frac{\mu_{hnf}}{\rho_{hnf}\alpha_f}\left(\frac{\partial^2 W}{\partial X^2}+\frac{\partial^2 W}{\partial Y^2}+\frac{\partial^2 W}{\partial Z^2}\right)-C_2(\frac{\mu_{hnf}}{\rho_{hnf}\alpha_f}\frac{U}{Da})$$
$$+C_2(\frac{(\rho\beta)_{hnf}}{(\rho\beta)_f}Ra*\theta+Ha^2*Pr*W \quad (10)$$

$$U\frac{\partial\theta}{\partial X}+V\frac{\partial\theta}{\partial Y}+W\frac{\partial\theta}{\partial Z}=\alpha^*(\frac{\partial^2\theta}{\partial X^2}+\frac{\partial^2\theta}{\partial Y^2}+\frac{\partial^2\theta}{\partial Z^2}) \quad (11)$$

The effective thermal diffusivity of porous medium is defined as follows.

$$\alpha_{eff}=k_{eff}/(\rho c_p)_{hnf} \quad (12)$$

$$k_{eff}=(1-e)k_s+e*k_{hnf} \quad (13)$$

Thermal diffusivity of hybrid nanofluid:

$$\alpha_{hnf}=\frac{k_{hnf}}{(\rho C_p)_{Al2O3-Cu/H2O}} \quad (14)$$

Brinkman [12] provided the effective dynamic viscosity of the nanofluid, and this equation is modified for use in hybrid nanofluids:

$$\mu_{hnf}=\frac{\mu_f}{(1-\emptyset_{Al2O3})^{2.5}(1-\emptyset_{Cu})^{2.5}} \quad (15)$$

Dynamic viscosity of hybrid nanofluid ($\emptyset_{hnf}=\emptyset_{Cu}+\emptyset_{Al2O3}$) is expressed as:

$$\mu_{thnf}=\frac{\mu_f}{(1-\emptyset_{hnf})^{2.5}} \quad (16)$$

The thermal conductivity of the hybrid nanofluid formula of Maxwell relationships is as [13]:

$$\frac{k_{hnf}}{k_{nf}}=\frac{k_2+(m-1)k_{hnf}-(m-1)\emptyset_2(k_{hnf}-k_2)}{k_2+(m-1)k_{hnf}+\emptyset_2(k_{hnf}-k_2)} \quad (17)$$

The density, specific capacity, volumetric expansion, and electric conductivity of hybrid nanofluid, respectively, can be expressed as:

$$\rho_{hnf}=\emptyset_{Al2O3}\rho_{Al2O3}+(1-\emptyset_{hnf})\rho_{bf}+\emptyset_{Cu}\rho_{Cu} \quad (18)$$

$$(\rho C_p)_{hnf}=\emptyset_{Cu}(\rho C_p)_{Cu}+(1-\emptyset)\left(\rho C_p\right)_{bf}+\emptyset_{Al2O3}(\rho C_p)_{Al2O3} \quad (19)$$

$$(\rho\beta)_{hnf}=\emptyset_{Al2O3}(\rho\beta)_{Al2O2}+\left(1-\emptyset_{hnf}\right)\rho\beta_f+\emptyset_{Cu}\rho\beta_{Cu} \quad (20)$$

$$\sigma_{hnf} = \sigma_f[\frac{\sigma\emptyset_{Al2O3} + \sigma\emptyset_{Cu} + \sigma_f\emptyset_{thnf} + 2\emptyset_{hnf}(\sigma\emptyset_{Al2O3} + \sigma\emptyset_{Cu} - \sigma_f\emptyset_{hnf})}{\sigma\emptyset_{Al2O3} + \sigma\emptyset_{Cu} + \sigma_f\emptyset_{hnf} - \emptyset_{hnf}(\sigma\emptyset_{Al2O3} + \sigma\emptyset_{Cu} - \sigma_f\emptyset_{hnf})}] \quad (21)$$

4. Boundary conditions of the present model

The current investigations boundary conditions are providing by the subsequent expression:

For cold sidewalls on the left and right: U=0, V=0, W=0,$\theta = 0$, and $\Phi = 0$ (22)

For all insulated walls(adiabatic): U=0, V=0, W=0, and $\frac{\partial\theta}{\partial n} = 0$, (23)

At four heating sources: U=0, V=0, W=0,$\theta = 1$, and $\Phi = 1$ (24)

$u_f = u_p, v_f = v_p, w_f = w_p, \theta_f = \emptyset_p$ (25)

On the all the interface $\frac{\partial u_f}{\partial x} = \frac{\partial u_p}{\partial x}, \frac{\partial v_f}{\partial x} = \frac{\partial v_p}{\partial x}, \frac{\partial w_f}{\partial x} = \frac{\partial w_p}{\partial x}, k_f\frac{\partial T_f}{\partial x} = k_p\frac{\partial T_p}{\partial x}$ (26)

4.1 Average Nusselt Number

The integral of the temperature flux through a wall is the definition of the average Nu. It expressed as follows for hybrid-nanofluid at heating block.

$$Nu_{ave=}\frac{k_{hnf}}{k_{bf}}\iint \theta\nabla de_x dxdz \quad (27)$$

5. Grid independent test and Validation

Using the commercial COMSOL6.0 software, extensive computational simulations are executed to evaluate the precision of the numerical results. The convection flow inside the enclosure was simulated using a 3D computational mesh. A portion of the mesh generated for the numerical simulation is depicted in fig.2, and Table 2 illustrates how choosing the right number of mesh elements affects the precision and effectiveness of the simulation results. Table 2 shows the appropriate mesh elements generated for this study.

Tabel.2

mesh elements generated for this study at Ra=10^6,Da=10^{-3},, δ=0.5,ε=0.4, ∅=0.04,Ha=20

Grid size	Domain elements	Boundary elements	Time	Nu nanofluid	Error%	Nu porous	Error%
G1	14012	2246	20	4.2577	----	7.9659	----
G2	69022	7238	53	4.8235	0.1173	9.0662	0.1213
G3	120616	10400	60	4.9284	0.0212	9.3420	0.0295
G4	319291	19704	161	5.1595	0.0447	9.7231	0.0391
G5	904343	45122	492	5.3757	0.0402	10.131	0.0289
G6	3613180	130918	3866	5.5681	0.0338	10.496	0.0347
G7	4608359	133552	5759	5.5713	0.00057	10.506	0.00095

The simulation was conducted from extra coarse mesh to extremely fine mesh in order to execute a mesh independence analysis. With 3613180 elements, we found that the numerical calculations are potentially mesh-independent. As the number of elements increases, the inaccuracy reduces.

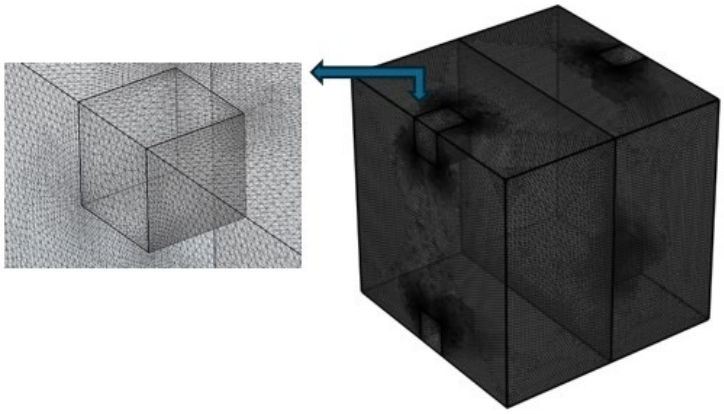

Fig.2 Mesh generation in the current study.

To validate the numerical simulation employed in the current study, natural convection flow within composite cavities filled with nanofluid (AL_2O_3- water) and porous medium was reported by Abeer **Alhashash** [14]. It was resolved by utilizing the same code employed in the current study. The parameters that selected for the comparison were Da=10^{-4} ,Ra =10^6, $R_k = 2, \emptyset = 0.05, and\ \delta = 0.25$. The outcomes indicate an excellent correlation between the current work and Alhashas [14], as shown in fig.3, adding to the confidence in the precision of the FEM solution currently being applied.

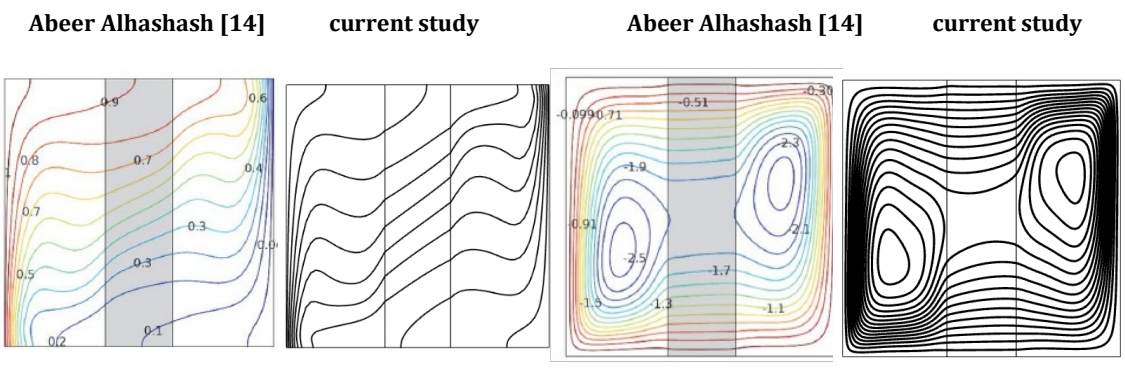

Fig.3 isotherms and streamlines for Ra=10^6,Porous layer thickness (δ=0.25),Da=10^{-4},, $\emptyset = 0.05$

6. Results and discussion

6.1 Effects of the Rayleigh number on the fluid motion and temperature field

Isotherms and streamlines are shown in fig.4 (a) to(b). Regarding all porous layer thicknesses, adding nanoparticles Cu (2%) and Al_2O_3 (2%) to the base fluid (pure water) causes the strength of the main streamlines cell to be stronger than that of the single-phase fluid. The reason behind this, the surface area of single-phase fluid that can be unitized for transferring heat is raised by adding Cu (2%) and (2%) Al_2O_3 nanoparticles. At low values of the Rayleigh number Ra= 10^3, the conduction in the system is predominant, and there is no convection movement. While the streamline patterns indicate cellular convection movement, they are relatively pointless due to the low flow gradient in contrast, there is less flow penetration into porous layer because of its resistance, restricting the flow from hybrid-nanofluid through the porous layer. Compared to hybrid nanofluid, single-phase fluid has more dominant circulation. Due to low Ra number observed in fig. 4 (a) which was triggered by the presence of nanoparticles making the fluid more viscous and decreasing the intensity of circulation. On the other hand, as the concentration of volume fraction for nanoparticles increase from ($\emptyset = 0,\ to\ \emptyset = 0.1$), there is a corresponding rise in circulation intensity due to thermal energy transfer throughout the flow associated with high concentration on nanoparticle movement. When the value of Ra increases to Ra=10^5, however, the convection movement starts and small arrows in the porous and hybrid-nanofluid layers begin to appear. Remarkably, convection movement is restricted to the fluid layer that lies on top of it, with a bit of penetration of convection occurring inside the porous porous-fluid layer. Consequently, penetrative convection is implicitly allowed. At high value of Rayleigh number (Ra=10^6), it is interesting to note that the velocities of the convection movement in the hybrid-nanofluid layer increase and enhance the velocity of flow penetration into the porous layer. The higher value of Ra leads to a change in the mode of thermal transfer within the enclosure from conduction to convection, because of increasing of the buoyancy force inside the enclosure. This helps decrease the temperature of the heat source by optimizing convection heat transfer. In the isotherms shown in fig.4 (a) to (c), the Rayleigh number plays a significant role in shaping form of the isotherms, it can be observed that at a low value of Ra=10^3 the heat transfer occurs in conduction mode. When the Ra number increases to Ra=10^5 the isotherm lines start to move from down of the enclosure to the top. It is interesting to observe that the temperature in the core of the enclosure begin to decrease gradually. This behavior is evident from the rapid rise of the cold zone within the enclosure. At higher value of Rayleigh number, converging isotherms lines are observed, increasing along the centerline of the enclosure. With a more rise in

Rayleigh number to (Ra=10^6), these converging isotherms lines become narrower, and the dominance of convection mode. These regions by dense isotherms in the boundary layer throughout the active sidewalls. There are additional mechanisms leading to the improvement of thermal transfer beyond the rise in effective conductivity of heat.

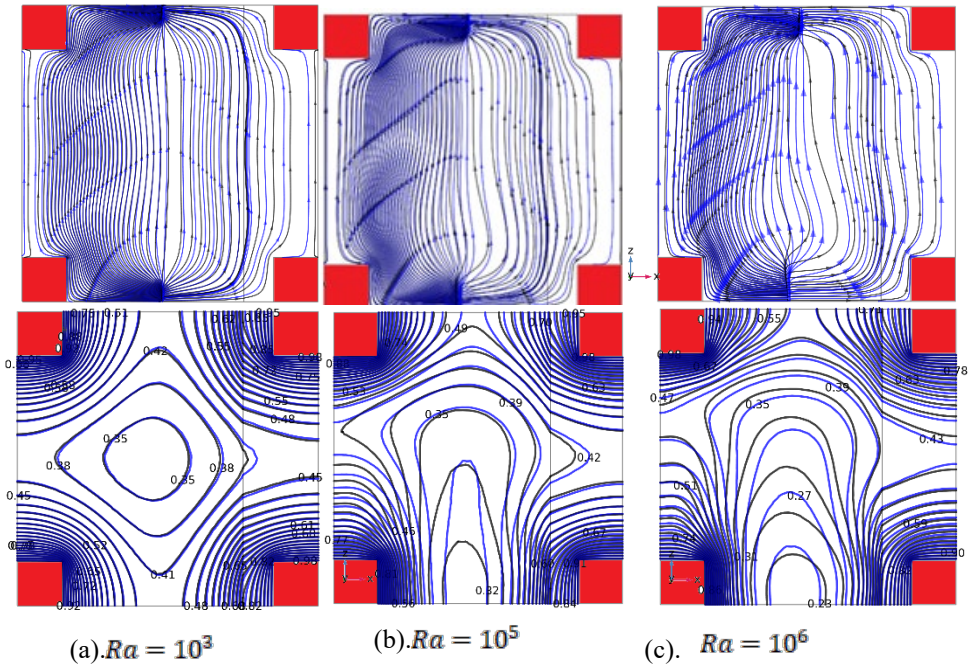

(a).$Ra = 10^3$ (b).$Ra = 10^5$ (c). $Ra = 10^6$

Fig.4 Streamlines (top) and isotherms(bottom) (a)-(c) porous layer thickness (δ=0.2), for different Rayleigh number at Ha=20, Da=10^{-3}, $\emptyset = 0.04$ blue color, while $\emptyset = 0$ black color, porosity e=0.4.

6.2 Effect of the Darcy number and porous layer thickness on the Average Nusselt number

Average Nusselt number versus (a) Darcy number and (b) porous layers thickness is shown in fig.5 for various parameter values for (a) Average Nu versus Da for three cases δ=0.2,δ=0.5,δ=1,at Ra=10^6,Ha=20,porosity=0.4,volume fraction ϕ=0.1, and (b) Average Nusselt number versus porous thickness for different Rayleigh number at Ha=20, volume fraction ϕ=0.1, porosity=0.4,Pr=6.2,Da=10^{-3}. At Darcy number (Da=10^{-5}) , it can be observed that average Nusselt number is at its lowest value . This is attributed to the small permeability of the porous medium, which prevents the hybrid-nanofluid from penetrating to the porous layer. The effect of the porous layer thickness can be clearly noted to have a significant impact on the Average Nusselt number, as the

rise in the porous layer thickness rise the flow resistance, thereby decreasing the rate of heat transfer. When the Darcy number is lower than (Da=10^{-4}), there is no obvious improvement, and the rate of heat transfer is not enhanced. It is interesting to note that the convection heat transfer begins when the Da $\geq 10^{-3}$. When increasing the Da number from 10^{-5} to 10^{-1}, there is noticeable increase in average Nusselt number for all porous layer thickness. Increasing Average Nusselt number at Da=10^{-1} is attributed to the increased permeability, which allows to the hybrid-nanofluid to penetrate to porous layer freely and accelerate the flow circulation. In fig.5 (b), the variation of the average Nusselt number with respect porous layer thickness for different Rayleigh number at Ha=20, volume fraction ϕ=0.1, porosity=0.4, Pr=6.2, Da=10^{-3}. The maximum value of average Nusselt number at Rayleigh number (Ra=10^{6}) for all the porous layer thicknesses. The convection heat transfer increase with an increase the porous layer thickness from 0.2 to 0.5, may be because there is more surface regime in the porous medium for heat transfer, which provides more heat exchanger between the hybrid-nanofluid and the solid matrix. The heat transfer is enhanced more pronouncedly, especially at $\delta = 0.5$.

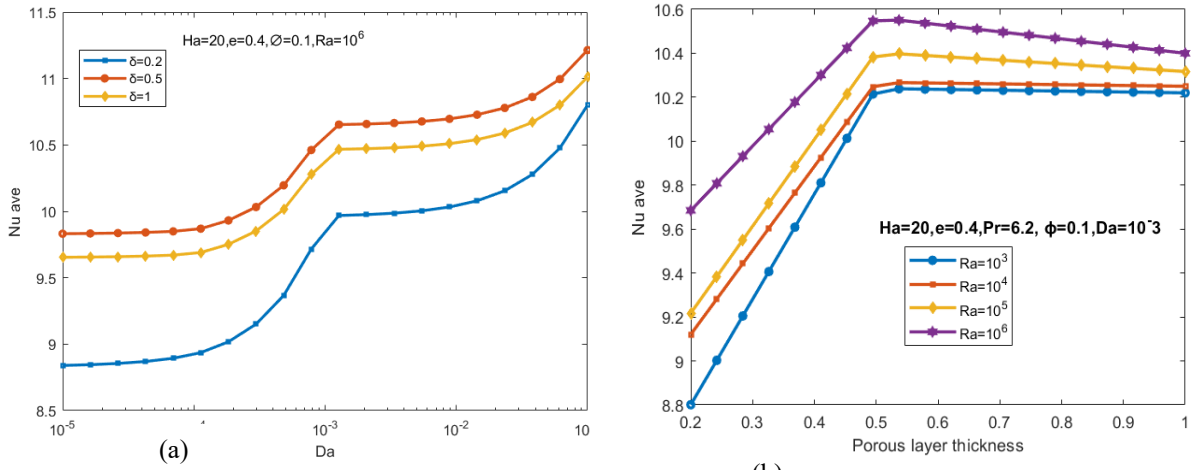

(a) (b)

Fig.5 Variation of the average Nusselt number with (a) Darcy number (b) porous layer thickness for three cases δ=0.2, δ=0.5, and δ=1, at Ra=10^{6},Ha=20, porosity=0.4, volume fraction of nanoparticles ϕ=0.1.

It can be noted that the average Nusselt number becomes almost constant with rising porous layer thickness up to $\delta = 0.5$. This behavior can be explained by lower penetration of streamlines associated with greater porous layer thickness and raised drag within the porous medium. Furthermore, there is an obvious rise in flow resistance, which reduces the average Nusselt number. Owing to higher

flow resistance that limits fluid movement and lowers convection heat transfer, this reduction occurs even though the surface area for heat transfer is greater.

6.3 Effect of the Rayleigh number and Hartmann number on the average Nusselt number

To reveal the impact of the Rayleigh number on the heat transfer properties of free convection in the hybrid-nanofluid enclosure filled partially with porous medium, in this section the Rayleigh number fluctuates within a range from $10^3 \leq Ra \leq 10^6$ for different solid volume fraction of nanoparticles at $\delta = 0.5, Da = 10^{-3}, Ha = 20, Pr = 6.2$. Fig.6(a) depicts the variation of the average Nusselt number on the heating block of the hybrid-nanofluid against Rayleigh number. It can be revealed that the average Nusselt number is a monotonically rising function of Rayleigh number. Increasing the nanoparticles in the hybrid nanofluid increases the average Nusselt number, due to improve the thermal conductivity. When the Rayleigh number rises, the hybrid-nanofluid moves more vigorously due to the rise in the buoyancy force, regardless of the solid volume of the nanoparticle's concentration.
In fig.6 (b) the average Nusselt number is plotted against the Hartmann number for different Rayleigh numbers, while other parameters are kept constant read as, $\delta = 0.5, Da = 10^{-3}, \phi = 0.1, Pr = 6.2$. The average Nusselt number rises greatly when the Rayleigh number increases from $10^3 to 10^6$. This is because, when the Rayleigh number increases, free convection increases dramatically due to the strong buoyancy impact. At a lower Rayleigh number, it can be observed that Hartmann suppression diminishes the effect of the Rayleigh number on heat transfer, due to the fact that buoyancy forces are not significant, and the magnetic field decreases the hybrid-nanofluid motion. The effect of Hartmann on the average Nusselt number becomes more significant when the Rayleigh number rises, and it becomes more noticeable. In this scenario, the convection effect is apparent. Consequently, it is easy to point out any rise in the Hartmann (magnetic field). This indicates that the Hartmann number reduces the average Nusselt number, and its influence becomes more pronounced at a greater value of the Rayleigh number. The Lorentz force can drastically change flow patterns by acting as a resistive force that opposes hybrid-nanofluid motion. Thus, it can be concluded that when a magnetic field does not exist, the average Nusselt number reaches its maximum value.

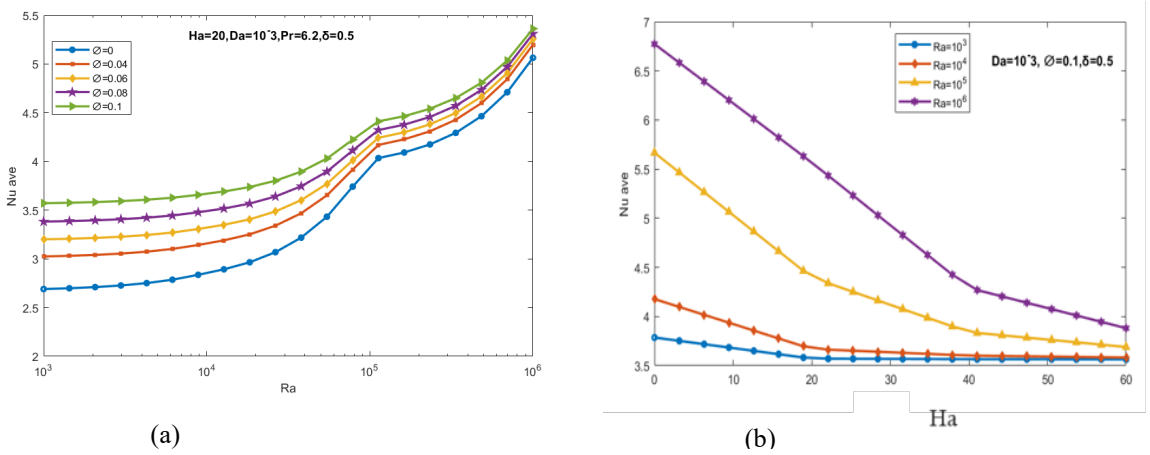

(a) (b)

Fig.6 Variation of average Nusselt number with (a) Rayleigh number (b) Hartmann number for different parameters at δ=0.5, Ha=20, , $\emptyset = 0.1$, and Prandtl number Pr=6.2.

7. Conclusions

In this study, numerical simulation of natural convection inside cubical enclosure filled with Al_2O_3-Cu base water hybrid-nanofluid partially saturated with porous medium have been carried out. The impacts of modified Hartmann number, Rayleigh number, solid volume fraction, and Darcy number were determined in terms of heat transfer rate, streamlines, and isotherms. The outcome of the numerical simulation has been summarized from the current study.

When the magnetic field (Ha) increases, the average Nusselt number decreases,
2.The temperature reaches its greater value when the magnetic field is absent (Ha=0).
3.The Nusselt number starts to decrease when the porous layer thickness increases more than (0.5).
4.The highest value of the temperature distribution is revealed at the core of the y-axis (y=0.5).
6.At Da=10^{-1},the hybrid-nanofluid penetrates to porous layer freely and accelerate the flow circulation, leading to an increase in the Nu, at Da=10^{-5}, the Nusselt number decreases.
7.Adding 10% of nanoparticles to pure water enhances the strength of circulation.
8.With an increase in porosity, the average Nusselt number decreases.

Nomenclature

Ra	Rayleigh number(Ra=Gr. Pr)
Da	Darcy number.

Ha	Hartmann number.
Pr	Prandtl number (Pr=.
B_0	magnetic field.
U,V,W	dimensionless velocity components in x, y, and z respectively.
u,v,w	velocity components in x,y, and z , respectively.
g,	acceleration because of the gravity (m/s^2).
p,	pressure (N/m^2).
P	dimensionless pressure.
Nu	Nusselt number, (Nu=h.L/k)
k_{hnf}	thermal conductivity of hybrid-nanofluid (w/m. K)
k_p	thermal conductivity of porous medium (w/m.K).
k_f	thermal conductivity of saturated fluid (w/m. K)
e	porosity of the porous medium.
δ	dimensionless porous layer thickness
Da	Darcy Number

REFERENCES

[1]. *Waini,I.; Ishak,A.;Pop,I*. Unsteady flow and heat transfer past a stretching /shrinking sheet in a hybrid nanofluid. Int. J. Heat mass Transfer.2019,136,288-297

[2].*S.U.S Choi*, Enhancing thermal conductivity of fluids with nanoparticles, ASME fluids Eng.Div.231(1995)99-105

[3]. Hemmat Esfe, M., Barzegarian, R., & Bahiraei, M. (2020). A 3Dnumerical study on natural convection flow of nanofluid inside a cubical enclosure equipped with porous fins using two-phase mixture model. Advanced Powder Technology. doi:10.1016/j.apt.2020.04.012.

[4]. *Kothuru Venkatadri, Syed Fazuruddin, Osman Anwar Bég & Obbu Ramesh (*2023) Natural convection of nanofluid flow in a porous medium in a right-angle trapezoidal enclosure: a Tiwari and Das' nanofluid model, Journal of Taibah University for Science, 17:1,2263224, DOI: 10.1080/16583655.2023.2263224

[5]. *Abderrahmane,A,Khetib Y,Ghodratallah ,P,Jasim ,j,D,Rawa , M,Qasem ,N,Younis ,O,Akbari ,O,Salahshou* ,S.Thermal performance of 3D Darcy-forchheimer porous rectangular wavy enclosures containing a water-Fe3O4 ferro-nanofluid under magnetic fields,53 (2024) 103790

[6]. *N, Muhammad and Naveed, A.* Method of moments solution to ethylene glycol based Al2O3 nanofluid flow through expanding/contracting rectangular channel ,Heliyon 9 (2023) e22415

[7]. *Aly, A. M.* (2020). Natural convection of a nanofluid-filled circular enclosure partially saturated with a porous medium using ISPH method. International Journal of Numerical Methods for Heat & Fluid Flow, 30(11), 4909–4932. doi:10.1108/hff-12-2019-0919

[8]. *Q. R. Al-Amir , H.K. Hamzah , F. H. Ali , M. H., W. Al-Kouz ,A. Al-Manea , R. Al-Rbaihatf, A.Alahmer*, Investigation of Natural Convection and Entropy Generation in a Porous Titled Z-Staggered Enclosure Saturated by TiO2-Water Nanofluid, Thermofluids 19 (2023) 100395

[9]. *N. K. Reddy ,H.A. K.Swamy ,M. Sankar , B.Jan*g, MHD convective flow of Ag–TiO2 hybrid nanofluid in an inclined porous annulus with internal heat generation, Thermal Engineering 42 (2023) 102719

[10]. *Gorla, R. S. R., Siddiqa, S., Mansour, M., Rashad, A. & Salah, T*., Heat Source/Sink Effects on a Hybrid Nanofluid-Filled Porous Enclosure. Journal of Thermophysics and Heat Transfer (2017).

[11]. *Thirupatithumma Anwar O, Reddy S. Sheri* finite differentially heated square enclosure utilizing nanofluids. Int. J Heat Mass Transfer. 2007; 50:2002-2018.

[12]. *Hughes T.J.R., Liu W.K. and Brooks A*., Finite Element Analysis of Incompressible Viscous Flow by the Penalty Function Formulation, Journal of Computational Physics, 30, 1979, pp. 1-60

[13]. *Maxwell, James Clerk,* A treatise on electricity and magnetism. Clarendon press, 1881

[14]. *Abeer Alhashash,* Free Convection Heat Transfer in Composite Enclosures with Porous and Nanofluid Layers, Article(2023) ID 2088607 | https://doi.org/10.1155/2023/2088607